IJCRT.ORG ISSN : 2320-2882

INTERNATIONAL JOURNAL OF CREATIVE RESEARCH THOUGHTS (IJCRT)

An International Open Access, Peer-reviewed, Refereed Journal

V_2O_5 doped Radiation shielding Efficiency of PbO-As_2O_3 glasses

P.Vijaya Lakshmi
Assistant Professor,
Department of Physics,
Sir.C.R.Reddy College Of Engineering (A),Eluru-534007

Abstract: The combination of fabricated glasses (40-x)PbO-60As_2O_3:xV_2O_5 doped with percentage levels up to 1mol% (i.e.X= 0.25, 0.50,0.75 and 1.0).The fabricated glasses prepared by standard melt-quenching technique. Phy-X proves to be an invaluable tool in the domain of radiation shielding.The linear attenuation coefficient (μ) exhibits a notable increase from 0.212 cm^{-1} for the sample(1.0 mol%) to 489.24 cm^{-1}. MAC indicates the lowest value(0.04) at elevated energy levels.The highest value 87.477 in at lowest energy level. The sample (0.25 mol%) exhibits the highest MFP, HVL, and TVL values, whereas the lowest values correspond to the sample (1.0mol%) doped with 1.0% V_2O_5. Z_{eff} values are high 52.97at high low energy level.N_{eff} values are high 5.17× 10^{23} at high low energy level. C_{eff} values are high 2.37× 10^{9}at high low energy level.

Index Terms - Radiation shielding parameters,Vanadium ions.

I. INTRODUCTION

In recent years, glass has garnered increasing attention as a viable and innovative alternative for radiation shielding applications, owing to its distinctive confluence of advantageous properties. One of its most compelling attributes is optical transparency, a feature that renders it exceptionally well-suited for environments such as radiological facilities where visual observation and monitoring are paramount. Additionally, the versatility of glass fabrication techniques—particularly the widely employed melt-quenching method—facilitates the tailoring of its structural and compositional characteristics. By manipulating its chemical constituents, the radiation attenuation performance of glass can be significantly optimized, thus extending its applicability across a broad spectrum of radiation protection contexts [1–3].These advantages have catalyzed a surge of scholarly interest and experimental investigations into the development of advanced glass-based shielding materials [4]. Radiation shielding materials are specifically engineered to attenuate ionizing radiation such as X-rays and gamma rays, thereby mitigating the adverse biological and environmental impacts associated with radiation exposure [5–7]. Historically, high-density materials such as lead and concrete have been the primary choices in this domain, owing to their proven efficacy in radiation attenuation [8,9].Lead, in particular, has been extensively studied due to its high atomic number and density, which confer superior shielding efficiency against a wide range of ionizing radiation energies [10,11]. However, its application is increasingly being scrutinized due to several critical limitations. These include its intrinsic toxicity, considerable weight, high procurement and handling costs, and a relatively low melting point that restricts its thermal stability [12]. Despite these drawbacks, lead oxide (PbO) remains noteworthy for its unique physicochemical properties, including a high refractive index, considerable mass density, favorable infrared transmittance, and pronounced nonlinear optical characteristics. These attributes have established PbO-based glasses as valuable materials not only in radiation shielding but also in optical and sealing applications.In clinical and diagnostic settings, lead-

containing glasses serve as essential protective barriers, safeguarding healthcare personnel from the deleterious effects of ionizing radiation during procedures such as radiography, fluoroscopy, and computed tomography. Lead-infused eyewear, for instance, constitutes a standard protective measure in radiological practices, playing a critical role in minimizing cumulative radiation exposure.Beyond lead-based systems, the incorporation of arsenic trioxide (As_2O_3) into glass matrices has demonstrated substantial potential in enhancing material performance. Functioning as a robust network former, As_2O_3 imparts a suite of superior physicochemical attributes when compared to more conventional borate- and phosphate-based glasses. These include a comparatively low melting temperature in the range of 550–650 °C, heightened thermal conductivity, and elevated thermal expansion coefficients. Moreover, As_2O_3-based glasses exhibit impressive resistance to moisture-induced degradation, a characteristic that enhances their long-term stability in diverse environmental conditions. These glasses are also recognized for their low optical losses and elevated Raman scattering efficiencies, rendering them particularly advantageous for use in optical communication systems and Raman-based amplification technologies [13 14].The present study systematically investigates the radiation shielding parameters of various glass compositions through the utilization of the Phy-X/PSD software platform, which offers a robust computational framework for evaluating photon interaction coefficients and related shielding metrics [15].

II. GLASS FABRICATION AND METHODS

V_2O5-doped PbO-As_2O_3 vitreous materials were synthesized employing the conventional melt-quenching methodology The molar concentration of V_2O_5 in the glass matrix was varied between 0.25 to 1.0 mol%. [16-18].A comprehensive listing of the glass compositions utilized in this investigation is presented in Table.1 The precursors for the fabrication of the glasses, including PbO,As_2O_3, , and V_2O_5 were all of analytical reagent grade (99.9% purity). These constituent compounds were meticulously homogenized in an agate mortar before being subjected to high-temperature melting in a silica crucible. The melting process was conducted in a furnace equipped with a proportional-integral-derivative (PID) temperature controller, maintaining a thermal range between 600°C and 650°C for approximately 30 minutes, ensuring the formation of a homogenous, bubble-free molten glass. The resulting melt was subsequently poured into a rectangular brass mold with a lustrous, velvety interior surface and allowed to cool to ambient temperature. Following casting, the samples underwent thermal annealing at 200°C in a separate furnace to relieve internal stresses. The glasses were then subjected to mechanical grinding and polished to achieve a mirror-like Glass.

III. Radiation Shielding Parameters

For the determination of the radiation attenuation coefficient, the Phy-X software[19].was employed. Phy-X proves to be an invaluable tool in the domain of radiation shielding, as it facilitates the calculation of attenuation parameters across a broad spectrum of energy ranges for a given sample. The software operates by incorporating the compositional data of the materials and their corresponding densities. Subsequently, the user can specify the desired energy range, either through a generalized spectral distribution or by selecting specific radioisotopes typically utilized in radiation attenuation studies. The linear attenuation coefficient (LAC or μ) constitutes a fundamental parameter in the analysis and design of radiation shielding materials. Its value can be quantitatively derived through the application of the Lambert-Beer Law, which characterizes the exponential attenuation of radiation intensity as it traverses an absorbing medium.

$$I = I_0 e^{-\mu x}$$

I denote the intensity of the attenuated ionizing photons, while I_0 signifies the intensity of the incident, non-attenuated ionizing photons. The symbol μ represents the linear attenuation coefficient (cm^{-1}), which quantifies the rate of attenuation per unit length. Additionally, x corresponds to the thickness (cm) of the material under investigation.

Fig. 1represents linear attenuation coefficient (LAC or μ) of fabricated glasses. The μ values for the dysprosium doped glasses are higher than that for the pure glass. The linear attenuation coefficient (μ) exhibits a notable increase from0.212 cm^{-1} for the pure glass to 489.84 cm^{-1} for the 1.0 mol% doped sample, spanning an energy range from 0.06 MeV to 0.01 MeV. This trend clearly indicates that the μ values for dysprosium-doped glasses are significantly higher than those for the pure glass, with the increase attributed to the enhanced density of the material. A similar pattern of behavior has been observed for these types of glasses in previous studies.

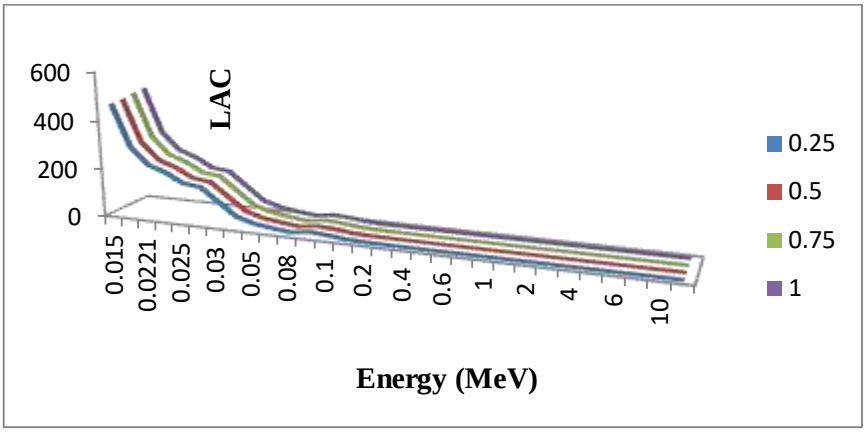

An additional attenuation parameter, known as the mass attenuation coefficient (MAC), quantifies the interaction probability of incident photons per unit mass of a material. This coefficient is determined by incorporating the density measurements of the sample. Notably, the values of the MAC were in complete concordance with those derived for the linear attenuation coefficient (LAC), thereby validating the consistency of the attenuation behavior across the sample materials.

$$\mu_m = \frac{\mu}{\rho}$$

Where μ_m is the mass attenuation coefficient (MAC) and ρ represents the material density.

Fig.2 illustrates the Mass Attenuation Coefficient (MAC) for the fabricated glass samples. The MAC values exhibit a discernible trend, commencing with the highest value observed in the pure (undoped) glass composition at lower photon energy levels, and progressively declining to the lowest value at elevated energy levels.The highest value 87.09 in at lowest energy level.

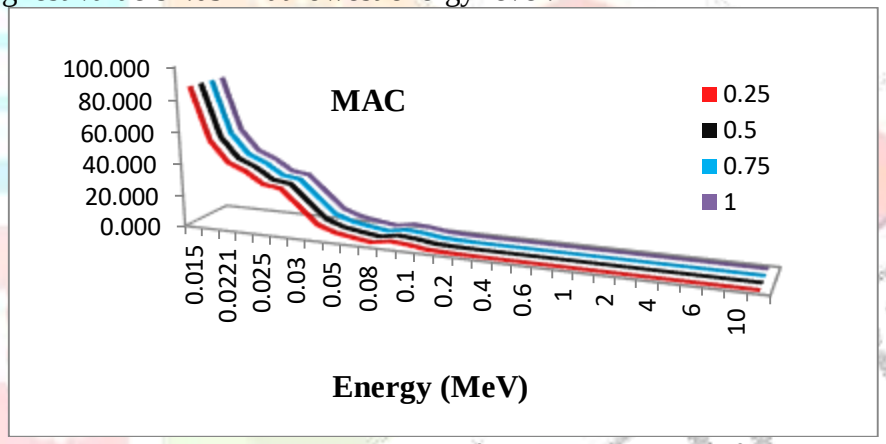

Figures 3, 4, and 5 delineate the variations in the mean free path (MFP), half-value layer (HVL), and tenth-value layer (TVL) parameters

The reciprocal of LAC is defined as the mean free path.

$$\mathbf{MFP} = \frac{1}{LAC}$$

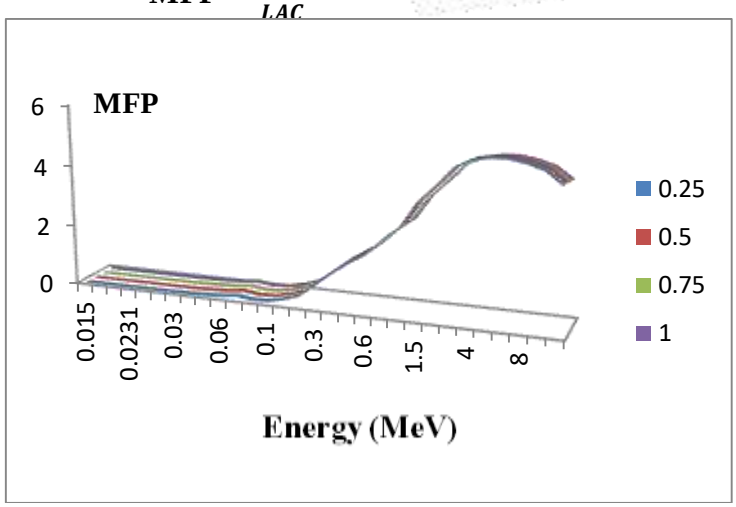

HVL is photon energy-dependent. The following formula is used for the evaluation of the HVL of any attenuator

$$\mathbf{HVL} = \frac{0.693}{\mu}$$

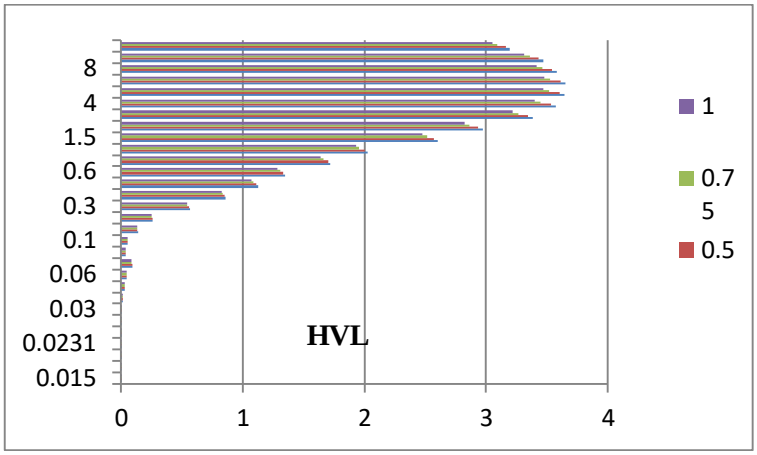

The thickness of the materials needed to shield most of the incoming photons (i.e., I0 becomes $0.1I_0$) is called the tenth value layer. Mathematically

$$\mathbf{TVL} = \frac{\boldsymbol{ln\ 10}}{\boldsymbol{LAC}}$$

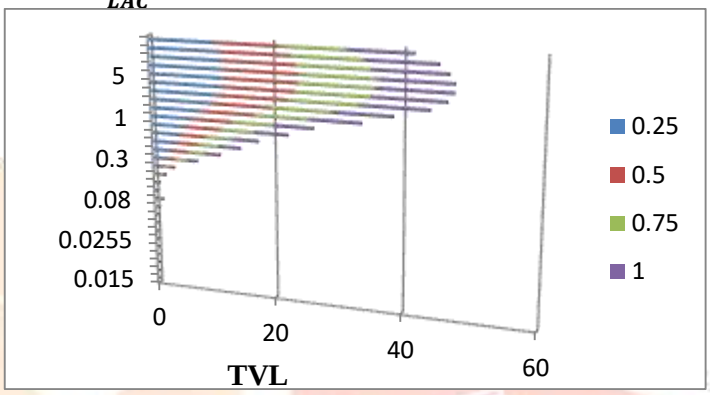

Figures 3,4 and 5 delineate the variations in the mean free path (MFP), half-value layer (HVL), and tenth-value layer (TVL) parameters for the fabricated glass samples.In generally observed for all samples,HVL >MFP> TVL at energy of the incident photons explained previous researchers The lowest HVL is 0.009 cm for SBTZBD6 at 0.02 MeV, the highest HVL was observed at 15 MeV with a value equal to 7.066 cm in this work the lowest HVL is 0.003 cm at 0.01 MeV, the HVL was observed at 10MeV with a value equal to 7.079.

The **effective atomic number (Z_{eff})** is a concept used to simplify the complex interactions of multiple elements in a glass. It represents an average atomic number that can be used to approximate the photon attenuation behavior in multi-element materials like glasses. Z_{eff} is especially useful when modeling radiation absorption and transmission. **Fig.6** represents the fabricated glasses clearly observed values are high 43.78×10^{23} at high low energy level.Previous study observed values high at low energy(Hammam Abdurabu Thabi et al., 2024).

$$\mathbf{Z_{eff}} = \frac{\sigma_a}{\sigma_e}$$

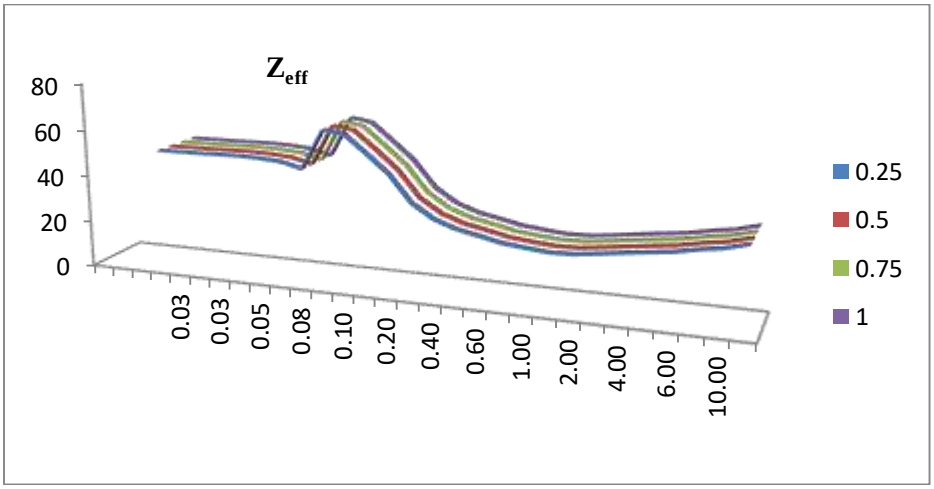

The **effective electron density (N_{eff})** represents the total number of electrons available for interactions per unit mass or volume. It plays a key role in photon attenuation calculations and is closely linked to Z_{eff}, since both are influenced by the elemental composition of the glass. **Fig.7** represents the fabricated glasses clearly observed values are high 5.152× 10^{23} at high low energy level.Similar values can be obtained BTD-Zn (R. Divina et al., 2020).

$$N_{eff} = \frac{\mu_m}{\sigma_e}$$

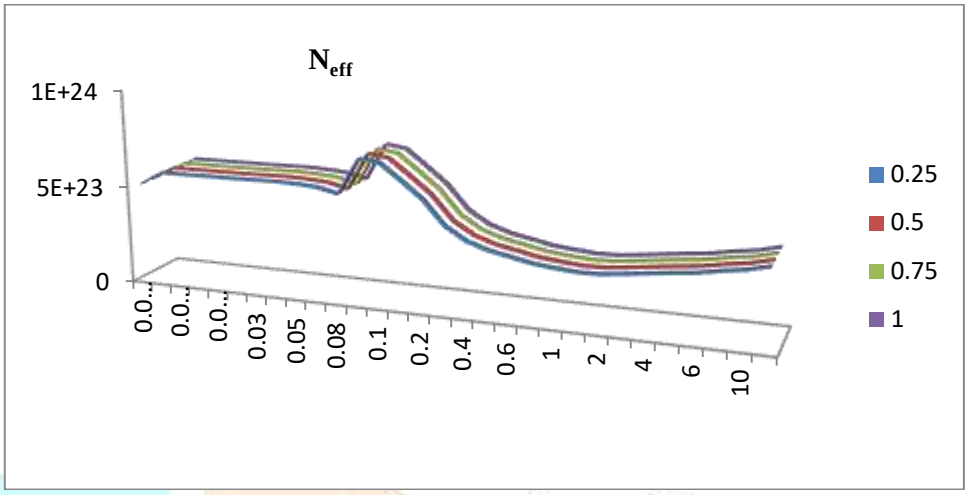

Lastly, **effective conductivity (C_{eff})** refers to the material's ability to conduct electric current, which is influenced by the mobility of charge carriers (such as electrons or ions) and their concentration. In glasses, this conductivity is typically low, but certain types of glasses (like ion-conducting or mixed network-forming glasses) can exhibit measurable conductivity. C_{eff} depends on factors such as temperature, glass composition, and the presence of specific conductive ions. **Fig.8** represents the fabricated glasses clearly observed values are high 1.09× 10^{8} at high low energy level.

$$C_{eff} = \left(\frac{N_{eff}}{m_e} e^2 \rho T \right) 103$$

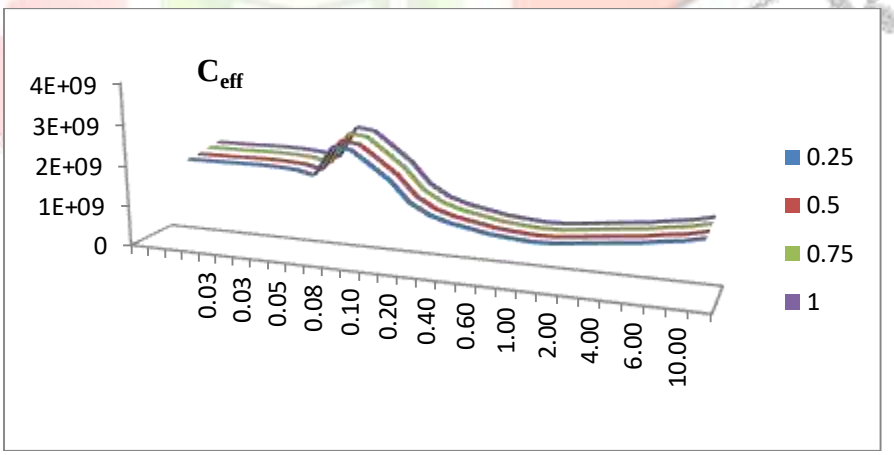

IV. Conclusions

The fabricated glasses prepared by standard melt-quenching technique. Phy-X proves to be an invaluable tool in the domain of radiation shielding.The linear attenuation coefficient (μ) exhibits a notable increase from 0.212 cm^{-1} for the sample(1.0 mol%) to 489.24 cm^{-1}. MAC indicates the lowest value(0.04) at elevated energy levels.The highest value 87.477 in at lowest energy level. The sample (0.25 mol%) exhibits the highest MFP, HVL, and TVL values, whereas the lowest values correspond to the sample (1.0mol%) doped with 1.0% V_2O_5. Z_{eff} values are high 52.97at high low energy level.N_{eff} values are high 5.17× 10^{23} at high low energy level. C_{eff} values are high 2.37× 10^{9}at high low energy level.

REFERENCES

[1].Bagheri, Reza, Alireza Khorrami Moghaddam, and Hassan Yousefnia. "Gamma ray shielding study of barium bismuth–borosilicate glasses as transparent shielding materials using MCNP-4C code, XCOM program, and available experimental data." Nuclear Engineering and Technology 49, no. 1 (2017): 216-223. https://doi.org/10.1016/j.net.2016.08.013.

[2].Saleh, Abdelmoneim. "Comparative shielding features for X/Gamma-rays, fast and thermal neutrons of some gadolinium silicoborate glasses." Progress in Nuclear Energy 154 (2022): 104482. https://doi.org/10.1016/j.pnucene.2022.104482.

[3].Abualsayed, Mohammad Ibrahim. "Radiation attenuation attributes for BaO-TiO_2-SiO_2-GeO_2 glass series: a comprehensive study using Phy-X software." Radiochimica Acta 111, no. 3 (2023): 211-216. https://doi.org/10.1515/ract-2022-0095.

[4]. Acikgoz, Abuzer, Gokhan Demircan, Demet Yılmaz, Bulent Aktas, Serife Yalcin, and Nuri Yorulmaz. "Structural, mechanical, radiation shielding properties and albedo parameters of alumina borate glasses: Role of CeO_2 and Er_2O_3." Materials Science and Engineering: B 276 (2022): 115519. https://doi.org/10.1016/j.mseb.2021.115519.

[5].Prasad, Rishu, Avinash R. Pai, S. Olutunde Oyadiji, Sabu Thomas, and S. K. S. Parashar. "Utilization of hazardous red mud in silicone rubber/MWCNT nanocomposites for high performance electromagnetic interference shielding." Journal of Cleaner Production 377 (2022): 134290. https://doi.org/10.1016/j.jclepro.2022.134290.

[6].Özdemir, Tonguç, and Seda Nur Yılmaz. "Mixed radiation shielding via 3-layered polydimethylsiloxane rubber composite containing hexagonal boron nitride, boron (III) oxide, bismuth (III) oxide for each layer." Radiation Physics and Chemistry 152 (2018): 17-22. https://doi.org/10.1016/j.radphyschem.2018.07.007.

[7]. Sayyed, M. I. "The role of Bi_2O_3 on radiation shielding characteristics of ternary bismuthtelluriteglasses."Optik270(2022):169973.https://doi.org/10.1016/j.ijleo.2022.169973.

[8].Naseer, K. A., K. Marimuthu, K. A. Mahmoud, and M. I. Sayyed. "Impact of Bi_2O_3 modifier concentration on barium–zincborate glasses: physical, structural, elastic, and radiation-shielding properties." The European Physical Journal Plus 136 (2021): 1-23. https://doi.org/10.1140/epjp/s13360-020-01056-6.

[9].Kim, Seulgi, Yunhee Ahn, Sung Ho Song, and Dongju Lee. "Tungsten nanoparticle anchoring on boron nitride nanosheet-based polymer nanocomposites for complex radiation shielding."CompositesScienceandTechnology221(2022):109353. https://doi.org/10.1016/j.compscitech.2022.109353.

[10].V.P. Singh, N. Badiger and J. Kaewkhao, Radiation shielding competence of silicate and borate heavy metal oxide glasses: Comparative study, J. Non-Cryst. Solids 404 (2014) 167.,https://doi.org/10.1016/j.jnoncrysol.2014.08.003.

[11].K. Singh, S. Singh, A. Dhaliwal and G. Singh, Gamma radiation shielding analysis of lead-flyash concretes, Appl. Radiat. Isot. 95 (2015) 174. DOI: 10.1016/j.apradiso.2014.10.022.

[12].B.A. Schueler, Operator shielding: How and why, Tech. Vasc. Intervent. Radiol. 13 (2010) 167.DOI: 10.1053/j.tvir.2010.03.005

[13]. G. Nagarjuna, T. Satyanarayana, V. Ravi Kumar, N. Venkatramaiah, P.V.V. Satyanarayana, N. Veeraiah, Spectroscopic investigations on PbO–As_2O_3 glasses crystallizedwithTiO_2,Philos.Mag.89(2009)22552270.https://doi.org/10.1080/14786430903049096

[14].K. Nassau, The material dispersion zero in infrared optical waveguide materials, Bell Syst. Tech. J. 60 (1981) 327–337.https://doi.org/10.1002/j.1538-7305.1981.tb00244.x.

[15]. K. Venkata Krishnaiah, P. Venkata Lakshmamma, C. Basavapoornima, I.R. Martín, K. Soler-Carracedo, M.A. Hernández-Rodríguez, V. Venkatramu, C.K. Jayasankar, Er^{3+}-doped tellurite glasses for enhancing a solar cell photocurrent through photon upconversion upon 1500nm excitation, Mater. Chem. Phys. 199 (2017) 67–72,https://doi.org/10.1016/j.matchemphys.2017.06.003.

[16].G. Ravi Kumar, T. Srikumar, G. Murali Krishna, G. Sahaya Baskaran, A. Siva Sesha Reddy, V. Ravi Kumar, C.S. Rao, The role of Ni^{2+} ions on structural and spectro scopic properties of Li_2O–ZrO_2–Y_2O_3–SiO_2 glass system, J. Non- Cryst. Solids. 498 (2018) 372–379. https://doi.org/10.1016/j.jnoncrysol.2018.03.025.

[17]. S. Thakur, A. Kaur, L. Singh, Mixed valence effect of Se^{6+} and Zr^{4+} on structural, thermal, physical, and optical properties of B_2O_3–Bi_2O_3–SeO_2–ZrO_2 glasses, Opt. Mater. 96 (2019),109338.https://doi.org/10.1016/j.optmat.2019.109338

[18].R.S. Omara , S. Hashima, S.K. Ghoshala , N.D. Shariff, Dose assessment of 4- and 16-slice multi-detector computed tomography (MDCT) scanners, Radiation Physics and Chemistry, https://doi.org/10.1016/j.radphyschem.2019.108445.

[19].NO.DANTAS.F.QU.J.T.ARNATES JR, EXPERIMENTAL STUDY OF ABSORPTION AND LUMINESCENCE PROPERTIES OF ER3+ IN LEAD SILICATE GLASS,J.ALLOYS COMPD.344 (2002) 316-319.HTTPS://DOI.ORG/10.1016/S0925-8388(02)00377-8.